Tectonic implications of fault-scarp–derived volcaniclastic deposits on Macquarie Island: Sedimentation at a fossil ridge-transform intersection?

Nathan R. Daczko[†]
Department of Geological Sciences and Institute for Geophysics, Jackson School of Geosciences, University of Texas, Austin, Texas 78712, USA and *GEMOC ARC National Key Centre, Department of Earth and Planetary Sciences, Macquarie University, NSW 2109, Australia*

Sharon Mosher[‡]
Department of Geological Sciences, Jackson School of Geosciences, University of Texas, Austin, Texas 78712, USA

Millard F. Coffin[§]
Ocean Research Institute, University of Tokyo, 1-15-1 Minamidai, Nakano-ku, Tokyo 164-8639, Japan

Timothy A. Meckel[#]
Department of Geological Sciences and Institute for Geophysics, Jackson School of Geosciences, University of Texas, Austin, Texas 78712, USA

ABSTRACT

Upper Miocene to lower Pliocene sedimentary rocks on Macquarie Island are dominantly volcaniclastic breccia, sandstone, and siltstone produced by the physical disintegration and tectonic abrasion of oceanic crust in fault zones and mass wasting of these tectonic features. They represent small debris fans and small-scale turbidites deposited at the base of active fault scarps, related to Late Miocene to Early Pliocene seafloor spreading. Most of the sediment is derived from basalts, but diabase and gabbro clasts in some sedimentary rocks indicate that middle and lower oceanic crust was exposed to erosion on the sea floor. A lack of exotic clasts and a low degree of clast roundness are consistent with a local source for the sediment and no input from continental rocks. Spatial relationships between sedimentary rocks and major faults associated with seafloor spreading on the island and correlation between sedimentary clast and adjacent up-thrown block compositions allow us to infer paleotectonic relief for Macquarie Island crust during deposition. Our data support a model involving the deposition of these rocks at the inside corner of a ridge-transform intersection. Furthermore, a tectonic reconstruction of the Australian-Pacific plate boundary for the approximate time that Macquarie Island crust formed (10.9 Ma) also shows that Macquarie Island crust most likely formed near a ridge-transform intersection. This paper describes sedimentation associated with active faulting at a ridge-transform intersection that has been uplifted in situ above sea level along with the surrounding oceanic crust, and demonstrates that high-angle faults have the most pronounced influence, compared with low-angle faults, on sedimentation in this tectonic environment.

Keywords: sedimentology, fault scarps, ridges, transform faults, Macquarie Island.

INTRODUCTION

Oceanic spreading ridges and associated transform faults are the most common type of plate boundary on Earth and represent sites of active tectonics, extensive magmatism, and crustal growth. The complex interplay between magmatism and faulting in the spreading-ridge environment creates relief. Active tectonics and irregular bathymetry combine to enhance the production, transport, and deposition of locally derived volcaniclastic sediments within a ridge and/or transform environment. Studies of sedimentary processes in spreading-ridge environments are hindered by limited subaerial exposures. Our knowledge therefore mainly comes from ophiolite settings (Bertrand et al., 1984; Lagabrielle and Cannat, 1990; MacLeod et al., 1990), supplemented by interpretations of dredged rock samples, shallow crustal drilling, and widely scattered submersible dives (Barany and Karson, 1989; Gallo et al., 1984; Karson and Dick, 1983; Karson et al., 1984; Mitchell et al., 2000).

The specific tectonic provenance of many ophiolite complexes is commonly obscured during dismemberment and translation of the oceanic crust to land (e.g., Simonian and Gass, 1978; Karson, 1984). In this regard, Macquarie Island, located ~1200 km southwest of New Zealand in the Southern Ocean (Fig. 1), is unique in that it is the only subaerial exposure of non-plume-related oceanic crust that still lies within the basin in which it formed. This provides a unique opportunity to carefully examine structures and sedimentary rocks on the island and to place these into a relatively well-constrained plate tectonic setting.

In this paper we examine sedimentary rocks on Macquarie Island and demonstrate a spatial relation between major seafloor spreading-related structures (onshore and offshore) and these exposures. On the basis of these data, we propose a model for the relation between faulting and sedimentation on Macquarie Island and show that these data support a model for formation and evolution of Macquarie Island at the inside corner of a ridge-transform intersection.

TECTONIC SETTING

Oceanic crust around Macquarie Island originated at three different seafloor spreading

[†]E-mail: ndaczko@els.mq.edu.au.
[‡]E-mail: mosher@mail.utexas.edu.
[§]E-mail: mcoffin@ori.u-tokyo.ac.jp.
[#]E-mail: tmeckel@usgs.gov.

GSA Bulletin; January/February 2005; v. 117; no. 1/2; p. 18–31; doi: 10.1130/B25469.1; 8 figures.

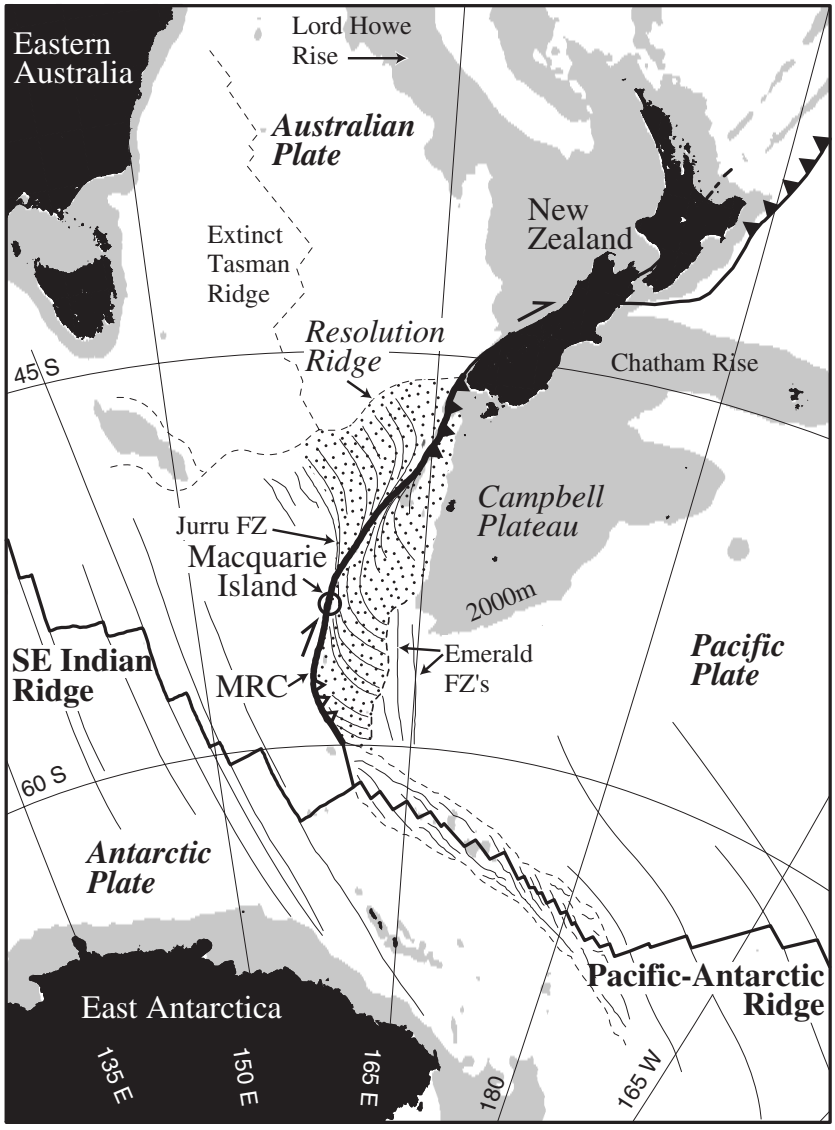

Figure 1. Location map of Macquarie Island and the Australian-Pacific transform plate boundary south of New Zealand. The thickest black line shows the extent of the Macquarie Ridge Complex (MRC). Crust formed by Australian-Pacific spreading along the (now extinct) Macquarie spreading ridge between ca. 40 and ca. 10 Ma is stippled. Filled triangles along the plate boundary are subduction zones; open triangles (in the Hjort region) represent incipient subduction (Meckel, 2003). Light gray illustrates regions ≤2000 m below sea level. Present plate boundaries are shown as black lines. Past plate boundaries are shown as dashed black lines. Fracture zones (FZ) are shown as thin black lines. Azimuthal equidistant projection centered at 60°S, 180°E (after Daczko et al., 2003).

systems, the Southeast Indian, Pacific-Antarctic, and Macquarie spreading ridges (Cande et al., 2000). The first two spreading centers are still active, whereas crust of the Macquarie region (shown stippled on Fig. 1) was generated at the (now extinct) divergent Australian-Pacific plate boundary following breakup between the Campbell Plateau and Resolution Ridge. Spreading occurred between middle Eocene (ca. 40 Ma) (Wood et al., 1996) and late Miocene time (Fig. 1; <10 Ma from the age of Macquarie Island crust) (Duncan and Varne, 1988). Fracture zones in the Macquarie-region crust curve and merge asymptotically into the active Australian-Pacific transform plate boundary, the Macquarie Ridge Complex (MRC; Fig. 1), consistent with progressive clockwise rotation of the spreading-ridge segments with time (Massell et al., 2000). The cumulative length of spreading segments along the plate boundary decreased relative to that of transform faults until spreading along the MRC ceased at <10 Ma. At that time, right lateral strike-slip faults began accommodating displacement along the transform plate boundary (Massell et al., 2000; Frohlich et al., 1997; Lamarche et al., 1997). Subsequent transpression across the Australian-Pacific transform plate boundary has led to deformation along the MRC resulting in a ridge and trough system (Massell et al., 2000; Meckel, 2003) and uplift of Macquarie Island.

The only subaerial exposure of the MRC is Macquarie Island and small adjacent islets, totaling 129 km^2, that protrude (maximum elevation 433 m) above sea level (Fig. 2). Macquarie Island is conformable with submerged oceanic crust directly east of the island, and marine geophysical data show a north-northeast-striking fracture zone ~7 km offshore, and west-northwest-striking spreading fabric (abyssal hill faults) (Massell et al., 2000; Bernardel and Symonds, 2001). In contrast, conjugate Macquarie spreading-center crust west of the island has been translated 230–290 km north (Daczko et al., 2003) during Neogene and Quaternary transform motion along the plate boundary that lies ~4.5 km offshore to the west of Macquarie Island (Fig. 2). Oceanic crust currently lying west of the island and plate boundary was created at the Southeast Indian Ridge and subsequently translated northward. Wertz et al. (2003) have recently proposed that the most significant spreading-related structure on Macquarie Island (the Finch-Langdon fault; Fig. 2) formed at the inside corner of a ridge-transform intersection. This model suggests that oceanic crust now exposed on Macquarie Island formed south of a west-northwest-striking spreading-ridge segment and directly west of a north-northeast-striking left lateral transform.

FAULTS

Macquarie Island exposes oceanic crust and uppermost mantle ranging from extrusive lavas and minor sedimentary rocks to sheeted dikes, gabbros, and serpentinized peridotites (Christodoulou et al., 1984; Goscombe and Everard, 1998; Varne et al., 1969; Varne and Rubenach, 1972; Varne et al., 2000). Recent, transform-related faults dissect the entire island, producing fault scarps and pull-apart basins (Daczko et al., 2003). Three major relict fault systems, associated with hydrothermal mineralization, and therefore most likely related to Late Miocene to Early Pliocene seafloor spreading, juxtapose different crustal levels (Fig. 2). Most clastic sedimentary rocks are located proximal to and southwest of these faults, and are interbedded with volcanic rocks.

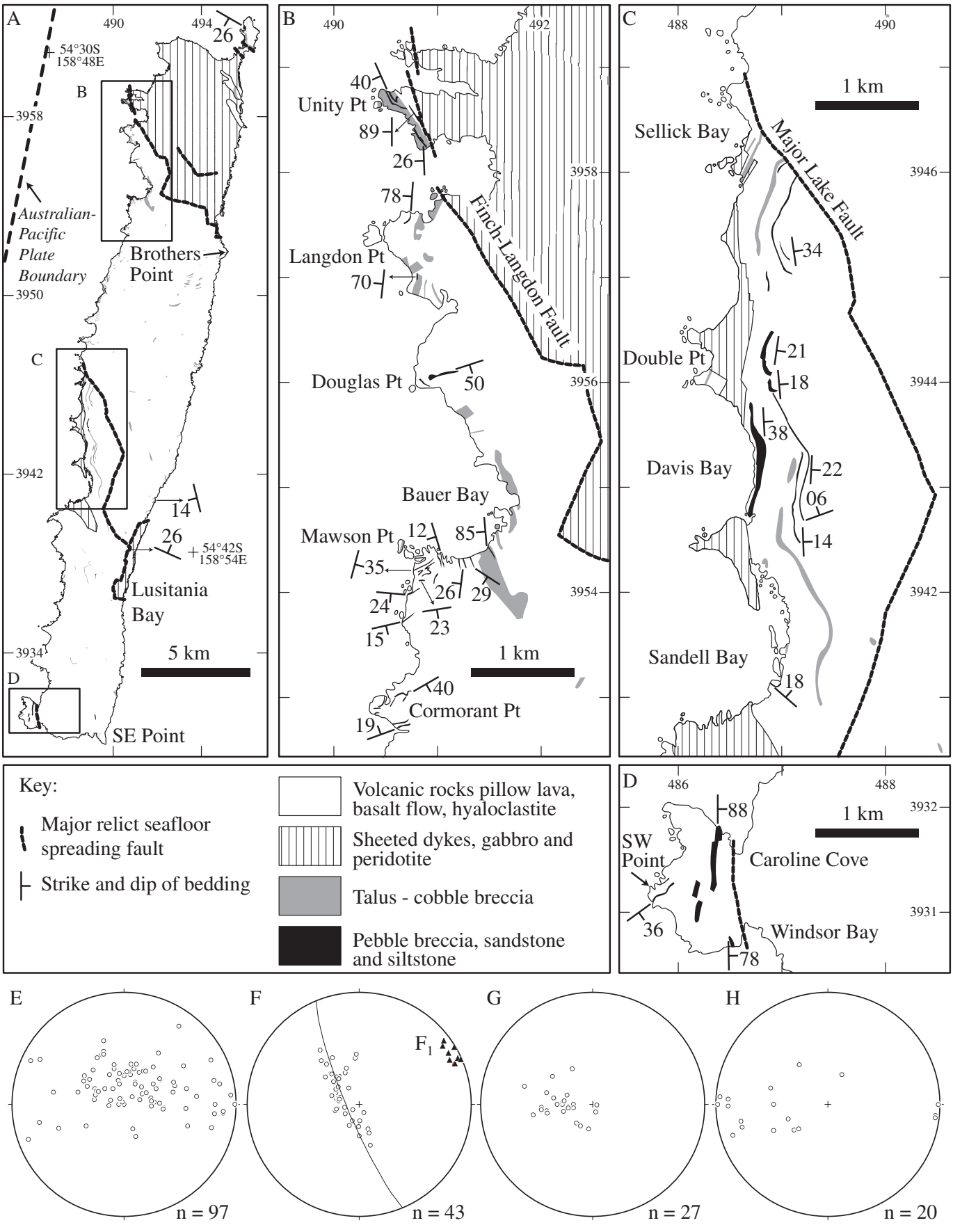
A
490
494
26
54°30S
158°48E
B
3958
Australian-
Pacific
Plate
Boundary
Brothers
Point
3950
C
3942
14
26
54°42S
158°54E
Lusitania
Bay
5 km
3934
D
SE Point
B
490
492
40
Unity Pt
89
26
3958
78
Finch-Langdon Fault
Langdon Pt
70
Douglas Pt
50
3956
Bauer Bay
Mawson Pt
12
85
35
26
29
24
23
15
3954
1 km
40
Cormorant Pt
19
C
488
490
1 km
Sellick Bay
Major Lake Fault
3946
34
Double Pt
21
18
3944
38
Davis Bay
22
06
14
3942
Sandell Bay
18
Key:
Major relict seafloor spreading fault
Strike and dip of bedding
Volcanic rocks pillow lava, basalt flow, hyaloclastite
Sheeted dykes, gabbro and peridotite
Talus - cobble breccia
Pebble breccia, sandstone and siltstone
D
486
488
88
1 km
3932
SW
Point
Caroline Cove
3931
36
Windsor Bay
78
E
n = 97
F
F1
n = 43
G
n = 27
H
n = 20

The Finch-Langdon fault juxtaposes lower-crust and upper-mantle rocks in the northeast with upper crust in the southwest and south (Fig. 2; see Wertz et al., 2003, for the latest overview of this structure). The fault comprises seven segments (0.5–2.25 km long) that strike either ~290°, ~340°, or ~20°; these form high-angle intersections with each other (Figs. 2A and 2B). On the basis of the juxtaposition of different crustal levels, the vertical displacement across the fault is more than a few kilometers. Discrete major faults are rarely observed; instead fault segments are defined by zones of fault gouge cemented by hydrothermal minerals and by numerous subsidiary faults parallel to the trace of the segments. The subsidiary faults dip steeply and generally have moderately to shallowly plunging slickenlines. Steeply dipping mylonites within gabbroic rocks adjacent and parallel to some fault segments have down-dip stretching lineations (Wertz et al., 2003). The hydrothermal mineralization includes epidote, prehnite, quartz, sulfides, carbonates, and zeolite. The thickest and most extensive clastic sedimentary sequences are located immediately southwest of the Finch-Langdon fault.

The long-lived Finch-Langdon fault displays early ductile fabrics that have been overprinted by brittle shearing. The later deformation dominates the fault zone, and samples of fault rock show abundant evidence of cataclastic deformation, distributed fracturing, and brecciation. Narrow fault zones (<100 mm wide) are defined by angular clasts of wall rock cemented by hydrothermal minerals (most commonly prehnite, but also epidote and quartz). Elsewhere, fracture networks and zones of cataclastically deformed rock commonly define the fault away from paths of hydrothermal fluids. An anastomosing spaced cleavage characterizes portions of the Finch-Langdon fault. Angular clasts of hydrothermal minerals are rarely cemented by a later phase of hydrothermal mineralization, attesting to some reactivation of the Finch-Langdon fault and reworking of older fault rock as the structure evolved. Thin sections of the Finch-Langdon fault (samples 17 and 18, Fig. 3), from Unity and Brothers Points, respectively (Fig. 2), are cataclastically deformed fault rock cemented by hydrothermal mineralization. Angular clasts of wall rock within the hydrothermal cements are indistinguishable from clasts within the sedimentary rocks described below. Individual clasts of wall rock are mostly basalt, but include diabase and gabbro where the Finch-Langdon fault cuts deeper crustal levels. Clasts rarely show internal deformation and are most commonly fractured.

Two other major faults related to Late Miocene to Early Pliocene seafloor spreading, the Major Lake and Caroline Cove-Windsor Bay faults (Fig. 2), show less apparent throw and less extensive adjacent sedimentary rocks. The Major Lake fault juxtaposes weakly metamorphosed volcanic rocks of different metamorphic grades (zeolite facies north of the fault and lower greenschist facies south of the fault) indicating a difference in crustal depths and merges with a fault that juxtaposes volcanic rocks and sheeted dikes near Lusitania Bay. The Caroline Cove-Windsor Bay fault juxtaposes volcanic rocks of the same apparent crustal level (both lower greenschist facies) but the fault and adjacent rocks are highly mineralized, primarily by quartz and sulfides.

SEDIMENTARY ROCKS

Sedimentary rock on Macquarie Island includes volcaniclastic pebble and cobble breccia, sandstone, siltstone, limestone, and rare chert. Angular clasts of coarse-grained sedimentary rock are commonly petrologically (texturally and mineralogically) similar across Macquarie Island (Fig. 3). Below we describe the field characteristics and broad petrologic character of the main lithologies. Given the coarse-grained nature of sedimentary rocks, flat-bed scans of polished thin sections best display textural variability amongst samples (Fig. 3; samples 1–16).

Pebble and Cobble Breccia

Breccia is immature, poorly sorted, and commonly massive (Fig. 4A), but may display crude stratification that is defined by preferential long-axis clast orientation (Fig. 4B). This lithofacies is the most volumetrically abundant on Macquarie Island and is composed of angular to subrounded clasts, mostly 20–150 mm in diameter, with rare blocks up to 400 mm across. We observe no systematic variation in clast size within or between deposits. Larger clasts are subrounded to angular (Fig. 5A), some possibly representing pillow shapes, whereas smaller clasts are more angular (Fig. 5B).

Across Macquarie Island, all clasts are derived from oceanic crust and breccia is commonly clast supported with a volcaniclastic matrix that is either fine-grained, green-gray sandstone or red sandy siltstone (Fig. 5A). Many clasts are tightly interlocking, consistent with compaction (Figs. 4C and 5A). Breccia is commonly oligomict, but nearly monomict pebble breccia with clasts dominantly derived from diabase dikes is found in the escarpment above Lusitania Bay adjacent to uplifted sheeted dikes (Fig. 2A). Pebble and cobble breccia is commonly overlain by finer-grained sedimentary rock that may show graded bedding (Fig. 4D and see below) or rarely this lithofacies may be capped by basalt flows.

In thin section, pebble and cobble breccia samples (samples 4, 7, 8, 14, 15, and 16; Fig. 3) are clast supported with a matrix of sand- and silt-sized volcaniclastic material and minor calcite cement. The matrix is commonly oxidized and may contain minor clay minerals (chlorite and/or illite and smectite). Clasts are commonly <20 mm, but may be up to 40 mm across (only the finer-grained components were sectioned; in outcrop clasts are up to 400 mm across). Clasts are most commonly basalt, but diabase is locally common (samples 4, 13, and 14). Gabbro clasts are exclusively observed in outcrop and samples from near the Finch-Langdon fault zone (Figs. 3 and 4C, sample 16). Most but not all samples contain clasts incorporating hydrothermal minerals and fault rock (samples 4, 7, 14, 15, and 16). One unusual section from float sampled ~1 km south of Mawson Point (sample 15; Fig. 3) almost exclusively contains clasts of hydrothermal minerals (mostly epidote and prehnite—light-colored grains labeled 'P' in Fig. 3). Very rare clasts of older sedimentary rock (sample 8) suggest minor reworking of older weakly lithified sediment in some areas.

Sandstone

Coarse to fine-grained sandstone commonly overlies breccia units (Figs. 4D and 4E), or directly overlies pillow lava or massive basalt flows (Fig. 4F). The contact between breccia and sandstone may be sharp (Fig. 4E) or gradational (Fig. 4D), and sandstone lenses a few tens of centimeters thick and a few meters wide

Figure 2. (A) Simplified geology map of Macquarie Island, showing major lithologic divisions and major relict seafloor spreading faults. (B) Geology map for Unity Point to Cormorant Point area SW of the Finch-Langdon fault. (C) Geology map for Sellick Bay to Sandell Bay area SW of the Major Lake fault. (D) Geology map for Caroline Cove area SW of the Caroline Cove-Windsor Bay fault. (E)–(H) Equal area lower hemisphere stereonet plots of poles to S_0 (open circles) for (E) Unity Point to Cormorant Point area, (F) Cormorant Point only, (G) Sellick Bay to Sandell Bay area, and (H) Caroline Cove area. Data from this study, supplemented with data from B. Goscombe (personal commun., 2003), and Goscombe and Everard (2001).

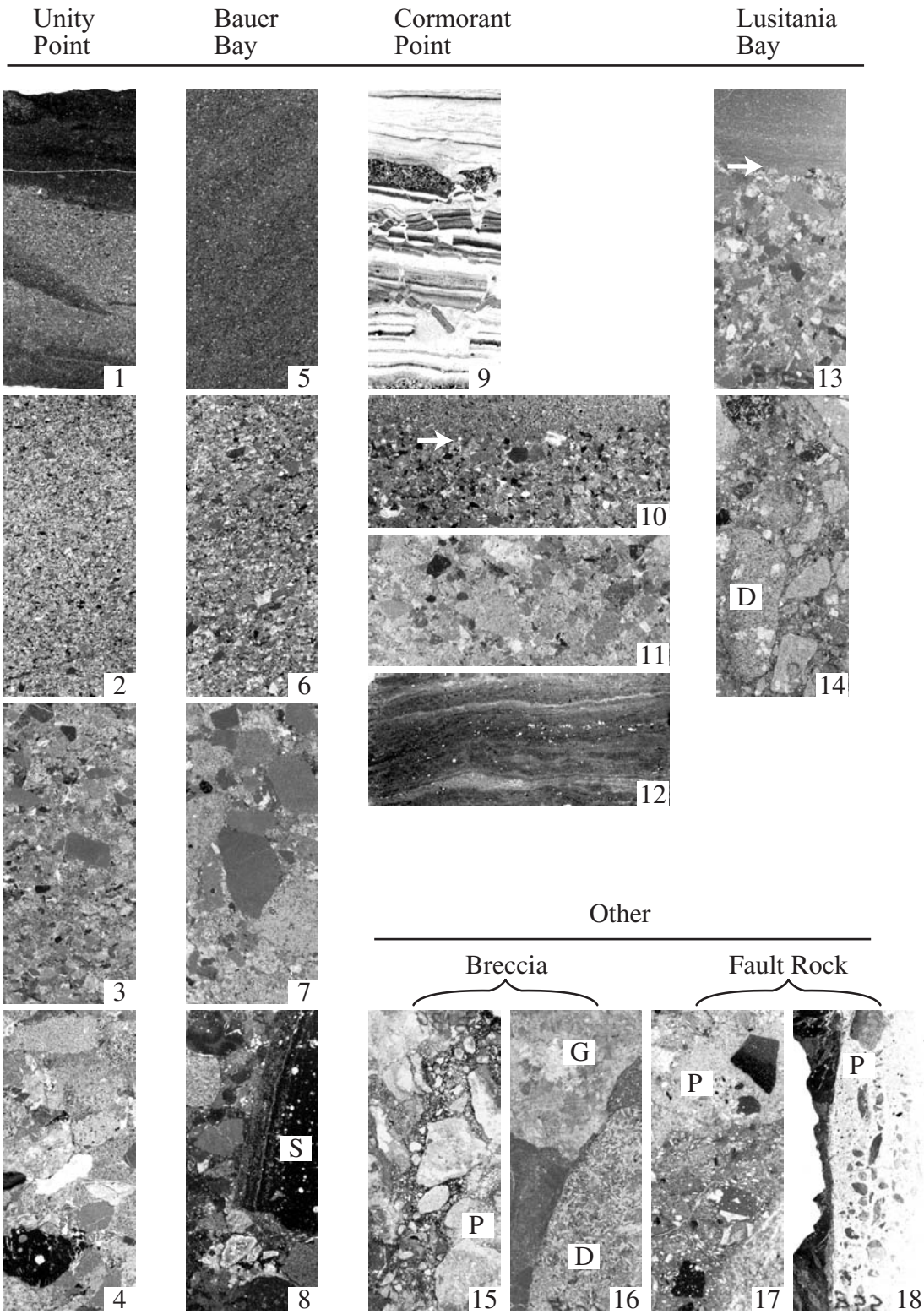

Figure 3. Flat-bed scans of thin sections for samples from representative stratigraphic sections (Fig. 6) showing textural variability within and between samples. S—sedimentary clast; P—prehnite clast or hydrothermal cement for samples 17 and 18; D—diabase clast; G—gabbro clast. Locations for samples 1–14 are keyed on Figure 6; other breccia samples 15 and 16 are float collected south of Mawson and Unity Points, respectively; Finch-Langdon fault samples for comparison are 17 and 18. Each section is ~35 mm long.

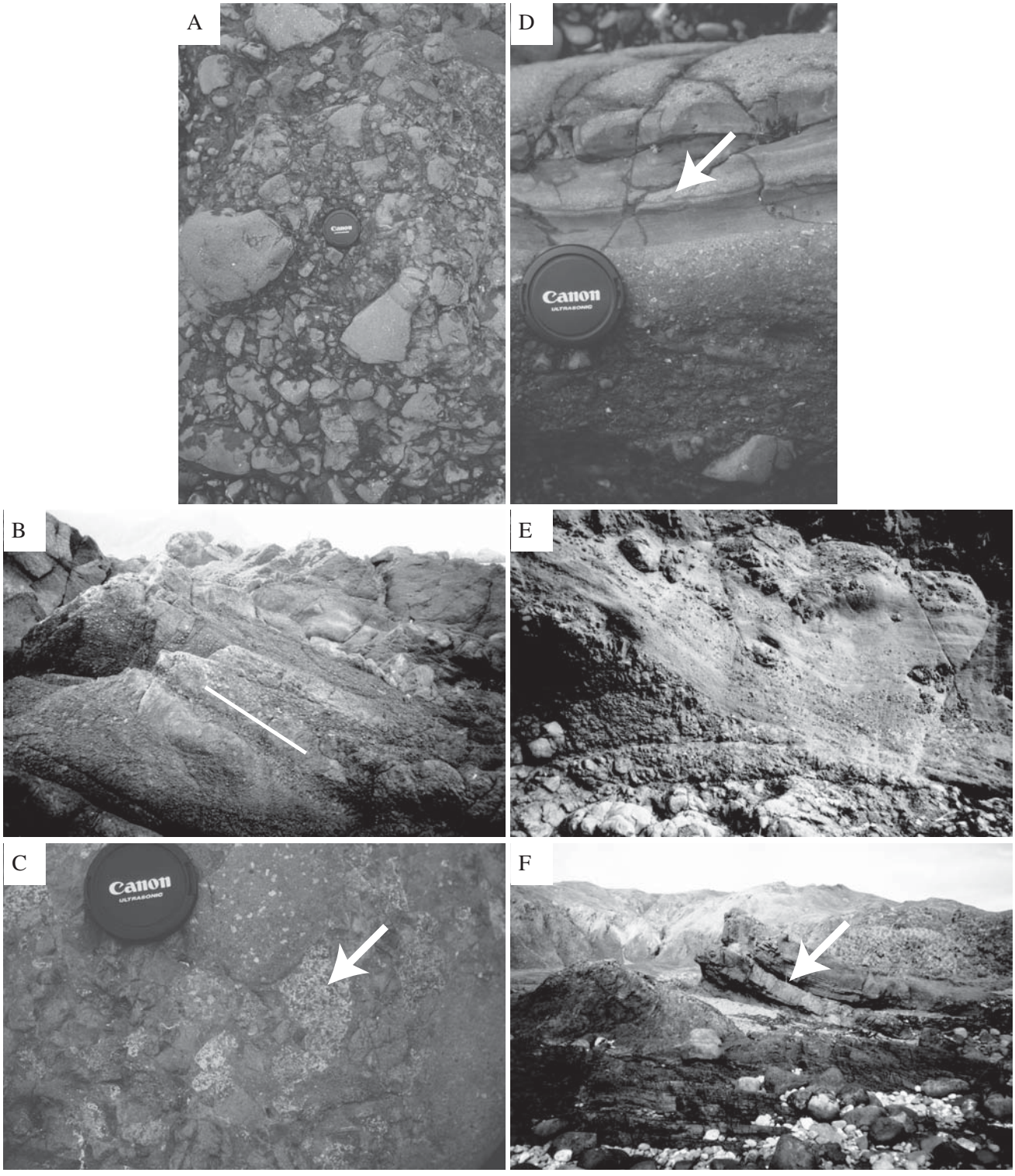

Figure 4. (A) Massive cobble breccia, Lusitania Bay. Lens cap is 60 mm across. Field of view is ~0.5 m. (B) Crudely stratified cobble breccia, Unity Point. White line indicates orientation of bedding. Field of view is ~5 m. (C) Pebble breccia with gabbro (white arrow) and diabase clasts, Unity Point. Lens cap is 60 mm across. Field of view is ~0.25 m. (D) Crudely stratified pebble breccia at base of photograph fining upward into well-laminated interbedded sandstone and siltstone, Caroline Cove. A second pebble breccia unit overlies siltstone at the top of the photograph. White arrow points to a flame structure. Lens cap is 60 mm across. Field of view is ~0.2 m. (E) Very poorly sorted sandstone with pebble and cobble clasts (20% gabbro), Douglas Point. The sandstone overlies pillow lava (lower left) and is overlain by basalt flow (upper right). Field of view is ~3 m. (F) Folded interbedded sedimentary rocks and basalt flows, Cormorant Point. White arrow points to basalt flow (~1 m thick). Field of view is ~20 m at the white arrow.

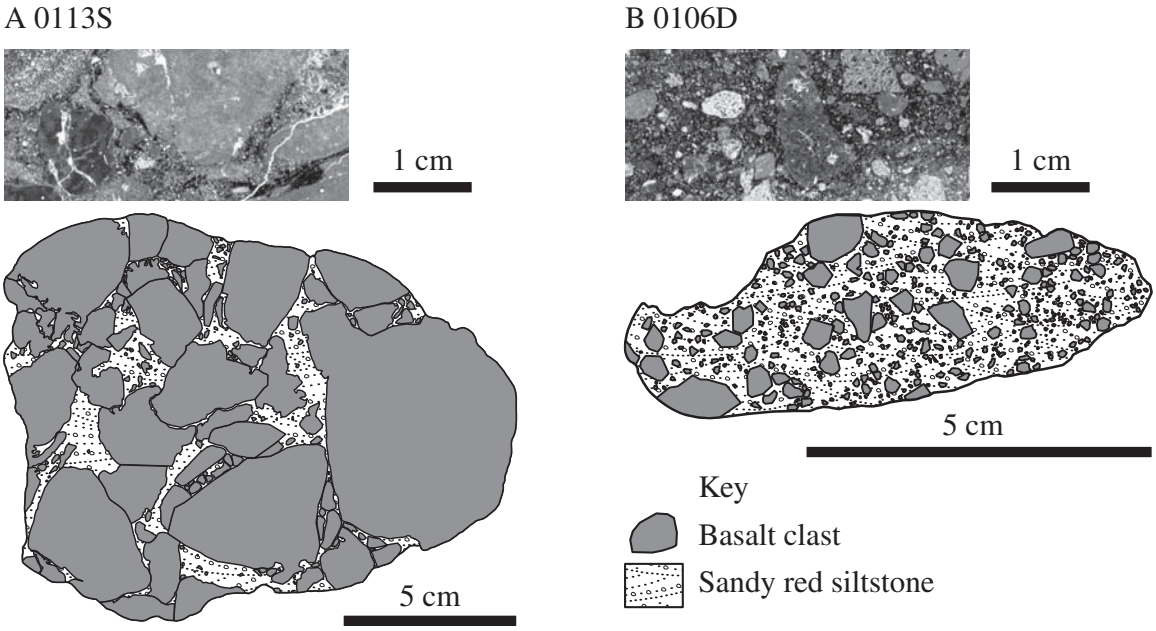

Figure 5. Flat-bed scan of thin section and cross-sectional hand sample sketch of cobble and pebble breccia samples (A) 0113S from Bauer Bay and (B) 0106D from Caroline Cove. Note the angular nature of clasts in 0106D.

are rarely observed within the breccia units. Sandstone is well indurated, immature, and commonly graded in 10–700-mm-thick fining-upward successions (Fig. 4D). Sandstone may also be interbedded with siltstone. Sandy layers are usually wedge shaped in outcrop (also sample 1, Fig. 3). Sandstone commonly grades upward into siltstone (Fig. 4D) and is overlain by more sandstone, or may be capped by basalt flow (Fig. 4F) or pillow lava.

Coarse to fine sandstone (samples 1, 2, 3, 5, 6, 10, 11, and 13; Fig. 3) is clast supported with minor silt-sized volcaniclastic material and cemented with microcrystalline carbonate (microspar). Sandstone may be gray-green or red, suggesting variability in the degree of oxidation of grains and matrix. The clasts are usually <1 mm across and well sorted. Sandstone is dominantly volcaniclastic with angular clasts and grains of lithic fragments or single minerals, some of which are recognizable in the field. Fragments are most commonly basalt, and single mineral grains usually include diopside or albite. Textural characteristics of diabase and gabbro are difficult to distinguish in finer-grained samples, even in thin section, but the coarse and pebbly sandstones contain diabase grains at Lusitania Bay, near the Major Lake fault, and gabbro grains at Unity Point/Douglas Point, near the Finch-Langdon fault (Fig. 2A). A very poorly sorted pebbly sandstone near the Finch-Langdon fault (Douglas Point) contains ~20% gabbro clasts (Fig. 4E). Medium-coarse pebbly sandstone samples (samples 3, 5, 6, 10, 11, and 13) commonly contain angular fragments of fault rock such as sheared, recrystallized, or cataclastically deformed wall rock (especially grains of albite or calcite with bent twins) and hydrothermal minerals such as epidote, prehnite, sulfides, spary calcite, and/or quartz. Petrologic identification of clasts of hydrothermal minerals or fault rock is difficult in fine sandstone samples.

Siltstone

Siltstone is less common than the coarser-grained sedimentary rocks and is usually found in association with sandstone (Fig. 4D). Sandstone lenses are also common within siltstone layers. Siltstone is commonly red, well indurated, immature, and generally found in layers less than a few centimeters thick, but also may be found as finely laminated beds <1 m thick. Siltstone comprises sheared, recrystallized, and cataclastic grains and exhibits parallel lamination and small-scale soft-sediment disruption features such as flame structures (Fig. 4D).

In thin section, all siltstone samples are homogeneous in color (commonly red and rarely green-gray) and texture and are very well sorted (uppermost part of sample 13; minor silt layers interbedded with chert, sample 9; Fig. 3). Petrologic identification of individual grains is difficult given the fine grain size; however, the grains appear the same as those identified in the sandstone (i.e., dominantly volcaniclastic).

Limestone and Chert

Across the island, minor pink limestone (interstitial to pillow lava) is common, and is also locally bedded with pillow lava as beds <0.5 m thick. The thickest bedded pink limestone (~0.5 m) is located on SW Point (Fig. 2D). Limestone is generally interbedded with pillow lava or basalt flow and rarely with volcaniclastic rocks. It commonly contains a very minor component of sand- or silt-sized grains of volcaniclastic material and is very well indurated. Foraminiferal outlines may be distinguished in thin sections of pink limestone (see below).

Rare chert is white to light gray in color and finely laminated. Nannofossil assemblages are poorly preserved and difficult to separate for identification due to the well-indurated nature of the rock. In thin section, the chert commonly contains minor silt or sand-size volcaniclastic fraction (sample 12) and is also interbedded with thin sand and silt layers (sample 9).

DISTRIBUTION OF SEDIMENTARY ROCKS

Sedimentary rocks, although widely distributed across Macquarie Island (Fig. 2A), crop out primarily toward the West Coast, with breccia and especially sandstone and siltstone being very rare on the East Coast. Furthermore, sedimentary rocks are concentrated in three locations along the West Coast: (1) Unity Point

to Cormorant Point, proximal to the Finch-Langdon fault (Fig. 2B); (2) Sellick Bay to Sandell Bay, proximal to the Major Lake fault (Fig. 2C; note minor sedimentary rocks are also associated with the extension of this fault to Lusitania Bay); and (3) in the Caroline Cove area, proximal to the Caroline Cove-Windsor Bay fault (Fig. 2D). Below we discuss each of these key areas. We have no data on interlayered sedimentary and igneous crust offshore.

Finch-Langdon Fault: Unity Point to Cormorant Point

The area proximal to the Finch-Langdon fault contains the largest volume and highest density of sedimentary rocks on Macquarie Island. The two largest deposits of cobble breccia are located at the SE corner of Bauer Bay (~170-m-thick unit) and on Unity Point (~80-m-thick unit; Figs. 2B and 4B). The highest density of finer-grained sedimentary rocks lies directly west of the Bauer Bay cobble breccia unit, along the southern shore of Bauer Bay, and out toward Mawson Point (Fig. 2B). The deposits extend 1–2.5 km away from the main trace of the Finch-Langdon fault. Overall, the strike of sedimentary bedding broadly follows the strike of the nearby segment of the Finch-Langdon fault and most sedimentary beds dip away from the fault zone. Sedimentary units generally dip shallowly, but show a broad range in orientations (Fig. 2E). Pebble and cobble breccia and sandstone contain clasts of deeper level rocks. Diabase is common in samples from Unity Point (sample 4; Fig. 3), gabbro clasts are found in samples from Unity (Figs. 3 and 4, sample 16) and Douglas Points, and most but not all samples contain clasts incorporating hydrothermal minerals and fault rock. Adjacent to the Finch-Langdon fault, rare limestone is interstitial to pillow lava, and the closest chert, also rare, crops out on Cormorant Point (2.5 km away).

On Unity Point immediately adjacent to the Finch-Langdon fault (Fig. 2B), four packages of sandstone and siltstone are interbedded with the ~80-m-thick cobble breccia unit (Fig. 4B) and another package lies between basalt flows (Fig. 6), stratigraphically below the cobble breccia unit, closer to the Finch-Langdon fault. The sandstone/siltstone packages are generally <3 m thick, most commonly contain 3–5 fining-upward cycles within an individual package (Fig. 6) and are concentrated toward the top of the cobble breccia unit. The combined thickness of sedimentary rocks on Unity Point is ~92 m, including the cobble breccia, and both breccia and sandstone contain diabase and gabbro clasts and grains. Although bedding can be difficult to distinguish within the cobble breccia unit, crude stratification suggests bedding planes dip ~35° toward the SW. Bedding within the sandstone and siltstone units is well defined, and these units dip ~25–40° toward the W and SW (Fig. 2B). Immediately adjacent to the fault, bedding is vertical to slightly overturned.

Further south at Douglas Point (~1 km from fault; Fig. 2B), very poorly sorted pebbly sandstone, containing ~20% gabbro plus some diabase clasts (Fig. 4E), overlies pillow basalt and is capped by a basalt flow or pillow basalt. The unit dips ~50° toward the S.

The most extensive sedimentary deposits on the island are located at and south of Bauer Bay. Of these, the coarsest grained are located most proximal to the fault and the units become progressively finer grained farther from the fault. The ~170-m-thick cobble breccia lies ~1 km from the fault trace, lacks clear internal stratification, and is interbedded with one package of finer-grained sedimentary rock that is nearly vertical. At least six other sedimentary packages are interbedded with extrusive lavas along the southern shore of Bauer Bay stratigraphically above the ~170-m-thick cobble breccia unit (Fig. 2B). Most of these packages are generally only a few meters thick. The combined thickness of sedimentary rocks along the southern shore of Bauer Bay is ~185 m, including the ~170-m-thick cobble breccia. A typical fine-grained package consists of a 1.5-m-thick cobble breccia unit overlying pillow basalt that fines upward into sandstone and siltstone and is capped by a basalt flow (Fig. 6). Siltstone at the top of one of these sequences contains flute casts elongate toward the SW, consistent with a NE-source region for the sediment (Fig. 6). The sedimentary packages at Bauer Bay dip most commonly 10–30° to the W and SW. At least four additional sedimentary packages are exposed on Mawson Point with a combined thickness of <10 m. These sedimentary rocks are similar in composition to those along the southern shore of Bauer Bay, but dip 15–35° toward the S and SE. At Cormorant Point, the sedimentary sequence most distal to the fault (~2.5 km) typically consists of finely laminated chert interbedded with volcaniclastic sandstone and siltstone (Fig. 6). The sedimentary bedding is openly folded about a subhorizontal F1 fold axis that plunges very shallowly toward the ENE (Fig. 2F), possibly repeating a <2-m-thick sequence of sedimentary rocks.

Major Lake fault: Sellick to Sandell Bays

The area proximal to the Major Lake fault contains the most laterally continuous sedimentary rocks on Macquarie Island (Fig. 2C). Fine-grained sedimentary rocks dominate the sequences here; cobble breccia units are (i) thinner (<20 m thick), (ii) rarely interbedded with finer-grained sedimentary rocks, and (iii) less common, compared to those adjacent to the Finch-Langdon fault. Some fine sandstone contains foraminifera, but chert and pure limestone are absent. At least ten fine-grained sedimentary packages are exposed with a combined thickness of ~60 m. In the escarpment directly east of Davis Point, a typical section shows seven ~20-cm-thick, fining-upward cycles of coarse-medium-grained sandstone interbedded with pillow lava (Fig. 6). Most sedimentary rocks are exposed within 1.5 km of the Major Lake fault trace. The strike of sedimentary bedding broadly follows the strike of the adjacent Major Lake fault zone and beds dip toward the fault zone, striking generally to the N to NNW and dipping shallowly to the E (Figs. 2B and 2G).

This fault merges with one near Lusitania Bay where an ~17-m-thick sedimentary package lies on the western side of the fault. This package dominantly consists of cobble breccia (~15 m thick) overlain by mainly siltstone interbedded with minor sandstone (Fig. 6). Much of the cobble breccia is monomict, containing only diabase clasts.

Caroline Cove–Windsor Bay Fault: Caroline Cove area

Only a short fault segment crops out between Caroline Cove and Windsor Bay, but the area to the west displays a significant volume of sedimentary rock and relationships that are similar to the two areas described above. All sedimentary rocks are within 500 m of the fault trace, before the SW coastline is reached. This area contains a single main sedimentary rock sequence—the thickest continuous package of pebble breccia, sandstone, and siltstone on Macquarie Island (~70 m thick). The package is dominantly pebble breccia, with thinner horizons of sandstone and siltstone showing graded bedding and flame structures (Fig. 6) that indicate younging toward the Caroline Cove–Windsor Bay fault. An ~1-m-thick finely laminated chert unit is also part of this package (Fig. 6). The top of the chert shows channel cut features and soft-sediment deformation including small-scale disruptions of bedding consistent with formation during deposition of the overlying pebble breccia unit. Soft-sediment folds are overturned toward the SW, again consistent with a NE source region for the overlying sediment. The thickest bedded limestone on the island (0.5 m; pink) is located in this area, on SW Point (Fig. 2D). Sedimentary bedding strikes north and dips near vertical adjacent to the Caroline Cove–Windsor Bay fault (Figs. 2D and 2H).

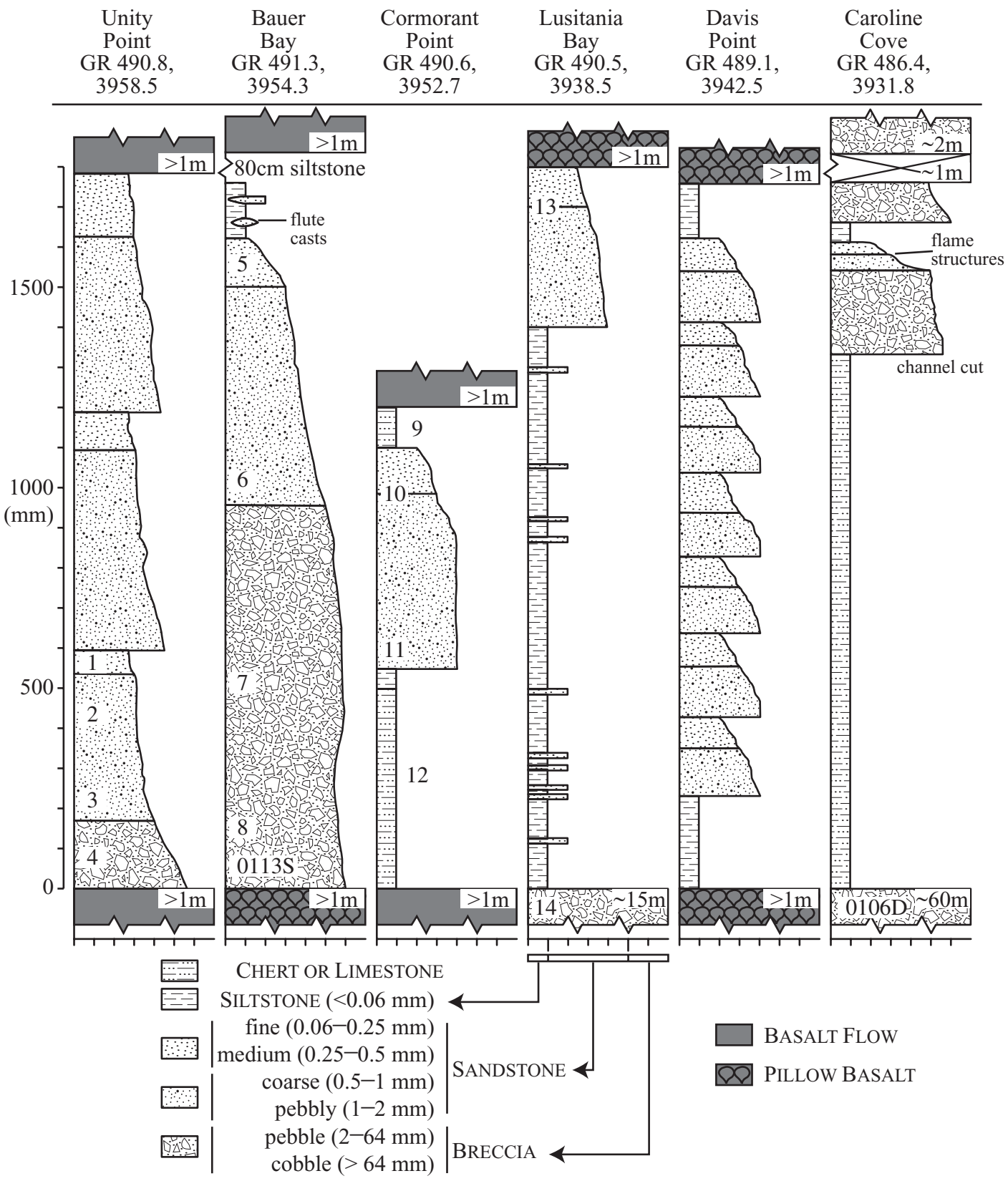

Figure 6. Representative stratigraphic sections from across the island; each section is only part of the total sedimentary rock from each area. The basalt flow at the base of the Unity Point section stratigraphically overlies an ~80-m-thick cobble breccia unit. The locations of samples 0113S and 0106D shown in Figure 5 are noted. Numbers represent the location of samples numbered 1–14 in Figure 3.

INTERPRETATION

Several observations lead us to conclude that most volcaniclastic sediment now lithified in sedimentary rocks SW of the Finch-Langdon fault was derived by physical disintegration and tectonic abrasion of oceanic crust within the Finch-Langdon fault or one of its accessory structures and mass wasting of these tectonic features: (i) sedimentary clasts of diabase and gabbro (e.g., Unity Point and Douglas Point) indicate that the lower-crust was exposed to seafloor erosion by the nearby Finch-Langdon fault zone; (ii) sandstone commonly contains angular fragments of fault rock such as sheared, recrystallized, or cataclastically deformed wall rock and hydrothermal minerals such as epidote, prehnite, sulfides, and/or quartz; (iii) angular fragments within the fault gouge are indistinguishable from clasts in the sedimentary rocks; and (iv) clast types and rare sedimentary structures such as flute casts are consistent with a NE provenance for sedimentary rocks SW of the Finch-Langdon fault. Furthermore, the fault has the largest throw (as evidenced by the juxtaposition of upper-mantle and volcanic rocks) and the thickest and most extensive sediments were deposited on the downthrown side. The other major relict seafloor spreading faults show a similar spatial relationship to the sedimentary rocks, contain only clasts exposed in the adjacent upthrown block, and show sediment transport to the southwest. The presence of massive basalt and pillow lava flows interbedded with the sedimentary rocks and diabase dikes that cut some sedimentary rocks indicates that deposition was concurrent with active volcanism.

The strike of the units generally parallels adjacent faults. Adjacent to the Major Lake and Caroline Cove–Windsor Bay faults, beds dip and young into the fault, suggesting the faults may be listric at depth. In contrast, the Finch-Langdon fault shows evidence of fault drag with sedimentary rocks dipping and younging away from the fault and locally rotated into a vertical to slightly overturned orientation adjacent to the fault. This geometry indicates high-angle faulting and activity after deposition of some units and is consistent with more significant throw on the Finch-Langdon fault than on the other two, potentially listric faults. No ultramafic clasts are observed within the sedimentary rocks, suggesting that either no ultramafic rocks were exposed at the time of sedimentation or that the serpentinized nature of the ultramafic rocks made them more susceptible to physical disaggregation and less likely to survive to form clasts. Ultramafic rocks crop out at the same topographic level as gabbroic rocks and proximal to them, suggesting that these units may have also been exposed.

Rock in the walls of some faults and reddish ferruginous siltstone show evidence of oxidation. We suggest that hydrothermal circulation on the seafloor caused at least some oxidation along faults and of fine-grained sediment prior to or shortly following sedimentation. Subaerial activity since uplift of the island may have also contributed to the oxidation. Some of the fine-sediment fraction, however, may be oxidized particles transported by air and ocean currents.

The similarity of clasts within fault gouge and adjacent sedimentary rocks is consistent with generation of much of the sediment in fault zones. The transport of sediment from fault scarps most likely involved gravity and/or tectonically induced slumping, debris slides, and matrix-poor debris flows (Lowe, 1982). The differences in grain size from cobbles to fine silt represent different degrees of physical degradation as a result of faulting and mass wasting. Much of the silt-sized fraction is most likely "rock flour" milled along fault scarps, then eroded. We propose that gravity-accentuated grain flows and small-scale turbidity currents were the dominant types of sediment gravity flow owing to the following observations: (i) sedimentary units are commonly normally graded from breccia to sandstone to siltstone; (ii) the graded bedding is commonly cyclic; and (iii) other sedimentary structures typical of turbidites include scour marks at the base of a deposit, flame structures, and laminated sand. Sedimentary units most commonly comprise poorly sorted, structureless breccia or sandstone overlain by laminated sandstone that may or may not be graded. These two layers compare well with the "a" and "b" layers of the Bouma division (Bouma, 1962). The "c" layer of the Bouma division was not observed, suggesting that the deposits are proximal to their source, as with increasing distance from the source, the deposits become finer as the coarse material is progressively deposited from a waning flow (Lowe, 1982).

Other sedimentary units consist of beds of poorly sorted, structureless, matrix-supported breccia and sandstone with or without a thin layer of siltstone at the top. These are most likely deposits of debris flows that contain a higher proportion of sediment in the mixture compared with "normal" turbidity currents, where most of the sediment carried is deposited simultaneously as a poorly sorted mixture, with only finer suspended material separating at the top of the flow (Lowe, 1982).

Limestone and chert are generally limited across the island and the maximum deposit thickness is ~1 m. These units most likely represent small sediment pockets isolated from tectonic sedimentation.

AGE OF SEDIMENTARY ROCKS

The sedimentary rocks on Macquarie Island are interbedded with pillow lavas and basalt flows and are therefore of similar age to the extrusive rocks. Isotopic dating of basalt from Macquarie Island yields $^{40}Ar/^{39}Ar$ plateau ages of 9.7–11.5 Ma (whole rock; Duncan and Varne, 1988) and ca. 6 Ma (glass; Wertz et al., 2002), giving middle to latest Miocene ages for formation of Macquarie Island crust. On the basis of *Globigerina* ooze that is interstitial to pillow lavas, Quilty et al. (1973) suggest an early (or perhaps middle) Miocene age of Macquarie Island crust.

We separated foraminifera and nannofossils from four samples of limestone and three samples of chert. All samples were very well indurated and both foraminifera and nannoplankton are very poorly preserved. The most useful foraminifera results (examined by P. Thompson, Plano, Texas) are from Davis Bay (sample 0226B; Fig. 2C). This sample contains *Globigerina bulloide*s d'Orbigny, *Globigerinoides trilobu*s (d'Orbigny), and sinistrally coiled *Neogloboquadrina pachyderma* (Ehrenberg). Aggregated, these give a late Miocene to Recent age. Nannofossil results (examined by W.H. Abbot, NannoChron International, Waxahachie, Texas; samples 0226B—Davis Bay and 0105C—Southeast Point) show *Coccolithus pelagicus* and possibly the variant *Coccolithus pliopelagicus*, which suggest a late Miocene or younger age. Some semicircular nannofossils tentatively identified as *Reticulofenestra pseudoumbilica,* an early Pliocene and older species, suggest a late Miocene to early Pliocene age for the samples.

PLATE TECTONIC RECONSTRUCTION

Our regional plate reconstructions use (i) the conjugate margins of the Resolution Ridge and Campbell Plateau and fracture-zone lineaments interpreted from regional gravity anomaly maps (Sandwell and Smith, 1997) and reflectivity data (Massell et al., 2000), and (ii) magnetic anomaly picks for the region (Weissel et al., 1977; Wood et al., 1996; Cande et al., 2000; Lawver et al., 2001; S.C. Cande, personal commun., 2002; W. Keller and J. Stock, personal commun., 2002; Cande and Stock, 2004). We used the Chron 5 old – C5o (10.9 Ma) finite-rotation pole determined for relative motion within the Australian-Pacific-Antarctic three-plate system (Cande and Stock, 2004). Finally we used the locations of magnetic anomaly picks and fracture zones to interpret the plate-boundary configuration for the time of the reconstruction (Fig. 7). The location of the easternmost Southeast Indian ridge is well constrained by magnetic data. The location of the Pacific-Antarctic transtensional boundary

is well constrained by the two ESE-trending conjugate margin lineaments shown. We inferred the orientations of spreading ridges and transform boundaries in the Macquarie region crust from the orientation of fracture zones and abyssal hill fabric that trend approximately N–S and E–W respectively. Without younger magnetic anomaly picks in the Macquarie region crust, the exact position of the spreading ridges and transforms in the Macquarie crust are open to interpretation, but we suggest that the overall geometry (Fig. 7) will not change dramatically as it is consistent with all available data. The sense of motion on the transform faults is right lateral for all transforms in the Macquarie crust except for the transform linking the Warna and Matata fracture zones (shown bold on Fig. 7), which is constrained to be left lateral on the basis on magnetic age data on either side of the Warna FZ (W. Keller and J. Stock, personal commun., 2002). This fracture zone lies offshore of Macquarie Island based on gravity and side-scan sonar data (Massell et al., 2002; Wertz et al., 2003). Wertz et al. (2003) propose that the Finch-Langdon fault and Macquarie Island crust formed at the inside corner of a ridge-transform intersection, adjacent to a left lateral transform. Our reconstruction shows that there was only one left lateral transform in this region, the one adjacent to the island, and we suggest that Macquarie Island crust formed at the ridge-transform-intersection inside corner, adjacent to it.

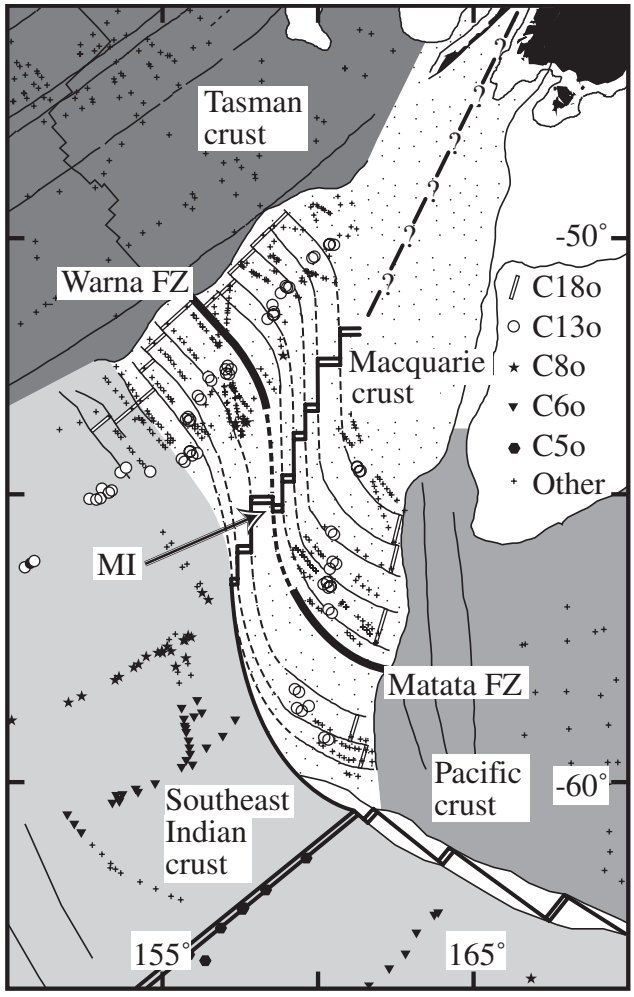

Figure 7. Plate tectonic reconstruction for Chron 5 old – C5o (10.9 Ma). Stippled crust formed at the Macquarie spreading ridge (now a transform boundary), light gray crust formed at the Southeast Indian spreading ridge (still active), medium gray crust formed at the Pacific-Antarctic spreading ridge (still active), and dark gray crust formed at the Tasman spreading ridge (extinct). Magnetic anomaly picks are represented by open circles (C13o, 33.3 Ma); filled stars (C8o, 26.6 Ma); filled triangles (C6o, 20.1 Ma); filled hexagons (C5o, 10.9 Ma); plus symbols (all other ages). Thin black lines are lineaments (continental margins and fracture zones) interpreted from the satellite-derived free-air gravity field (Sandwell and Smith, 1997). Medium black lines are the plate boundaries active at 10.9 Ma (double line = spreading ridge; single line = transform). Thickest black lines are the Warna (Australian plate) and Matata (Pacific plate) fracture zones (FZ). These two fracture zones are linked by the only left lateral transform fault within the Macquarie crust as shown by the offset of C18o picks (open rectangles). The dashed lines show our interpreted position of the fracture zones allowing for a minor component of deformation of the fracture zones during Neogene and Quaternary transpression along the Australian-Pacific plate boundary. The arrow points to the inside corner of the ridge-transform intersection where we interpret the crust of Macquarie Island (MI) most likely formed.

MODEL AND DISCUSSION

Clasts in sedimentary rocks from Macquarie Island indicate that basic extrusive rocks, sheeted diabase dikes, and gabbroic rocks were exposed to seafloor erosion by faulting. Field relationships show contemporaneous faulting, volcanism, and sedimentation, indicating that deep levels of oceanic crust (down to at least diabase and gabbro, and perhaps ultramafic rocks) were exposed during active tectonics near to a ridge environment. Sedimentary rocks on Macquarie Island are commonly covered by basalt flows or pillow lava, and dikes cut some breccia units. The sedimentary rocks are cut by faults and experienced high-grade seafloor alteration. Therefore, exhumation of lower oceanic crust adjacent to the Finch-Langdon fault occurred well before Macquarie Island (and the Macquarie Ridge Complex, MRC) was uplifted to its current elevation above the surrounding seafloor. The relief associated with sedimentation formed in response to the tectonic setting of Macquarie Island crust as it was forming.

We propose that seafloor-derived sediment was shed from a series of major submarine fault scarps in an inside corner of a ridge-transform intersection (Fig. 8). Data from active ridge-transform intersections suggest that the inside corner: (i) is elevated 0.5–1.5 km above conjugate outside corners (Severinghaus and MacDonald, 1988); (ii) has an elevated Bouguer gravity anomaly that suggests thinner crust (Tucholke et al., 1998); (iii) commonly exposes deep-crustal and mantle rocks (Karson and Dick, 1983; Cannat, 1993; Schroeder et al., 2002); and (iv) has normal and oblique faults with larger spacing (Karson and Dick, 1983). Corrugated domed massifs characterize

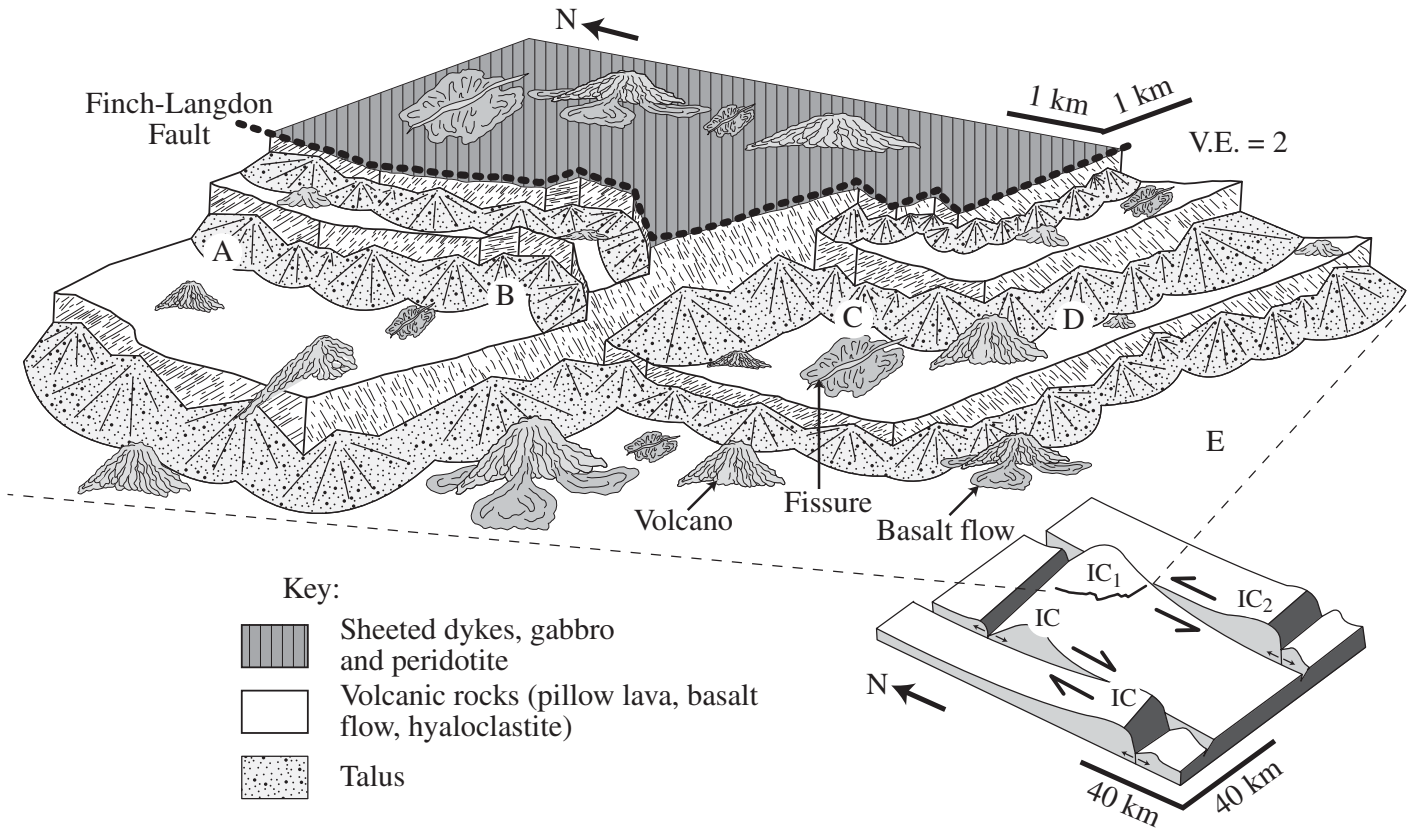

Figure 8. Model (ca. 10 Ma, V.E. = 2) of the Finch-Langdon fault (dashed line) and surrounding crust interpreted as an inside corner (IC) structure (inset after Tucholke and Lin, 1994). Shaded crust NE of the fault comprises sheeted dikes, gabbro, and peridotite. White benches, of lower relief, comprise volcanic rocks (pillow lava, basalt flow, hyaloclastite). Fault scarps show striated surfaces. Sediment wedges comprise sediment produced by the physical disintegration and tectonic abrasion of oceanic crust in submarine fault zones. Younger volcanic edifices and basalt flows that cap some sedimentary rocks are represented by volcanoes, associated flows, and massive basalt flows erupted from fissures. Volcanic activity interpreted to be related to a spreading-center located a few kilometers to the north (see inset, location IC_1) or to the south (see inset, location IC_2). Location "A" represents our interpretation of the setting of deposition of samples taken from Unity Point; "B" represents Douglas Point; "C" represents Bauer Bay; and "D" represents Mawson Point and Cormorant Point; "E" represents the small pockets of limestone or chert isolated from tectonic sedimentation (see Fig. 2 for location, and Figs. 3, 4, 5, and 6 for lithologic and stratigraphic descriptions).

many inside corner highs, as shown by bathymetric and side-scan sonar images; these have been interpreted as oceanic metamorphic core complexes (Cann et al., 1997; Tucholke et al., 1998). In addition to the development of core complexes, high-angle faults are observed (e.g., Karson and Dick, 1983) that appear to cut the detachment faults (Thy and Yildirim, 2000; Blackman et al., 1998; Lagabrielle et al., 1998). Models for these structures propose that they form within an inside corner in response to tectonic motion on the spreading ridge interacting with the motion on the transform fault, resulting in a complex array of structures that form parallel to the spreading ridge, parallel to the transform fault, and oblique to both (Allerton and Vine, 1992; MacLeod et al., 1990; Fox and Gallo, 1984; Moores and Vine, 1971).

On the basis of marine geophysical data to the east of Macquarie Island combined with new data from the island, Wertz et al. (2003) have proposed that the Finch-Langdon fault formed within an inside corner of a ridge-transform intersection, placing the Finch-Langdon fault into a larger oceanic tectonic context. Some Finch-Langdon fault segments parallel the offshore, relict transform fault (fracture zone oriented N–NE), some parallel the relict-spreading-center (spreading fabric oriented W–NW), and others are oblique to both (NW). Wertz et al. (2003) assumed that the ridge was located north of the crust making up the island, although the same structures would have formed with a ridge to the south, if the island's crust were on the opposite side of the left lateral transform (compare positions IC_1 and IC_2 in Fig. 8 inset). Either interpretation suggests that deeper crustal rocks exposed NE of the Finch-Langdon fault were exhumed in an inside corner setting and these units would have formed a bathymetric high capable of shedding sediment. Depending on the location of the ridge, sediment was shed westward or eastward into the transform valley, southward or northward into the spreading-ridge rift valley, and southwestward either toward the ridge-transform intersection as observed by Blackman et al. (1998) or away from the ridge transform intersection. Given the abundance of extrusive lava interbedded with the sedimentary rocks, a ridge to the south (either originally or from later ridge propagation as proposed by Wertz, 2003) seems most likely; in this case most sediment would have been transported toward the ridge-transform intersection. We

cannot rule out, however, that the bulk of the sediment transport was away from the ridge-transform intersection (i.e., ridge to the north). Regardless, our data and observations support the interpretation of the Finch-Langdon fault as an inside corner structure (Wertz et al., 2003), and these unique, above-sea-level exposures demonstrate the nature of such sedimentary sequences and the spatial relationships to the associated faults.

As discussed above, many inside corners expose major detachments along which deep crust and mantle rocks have been exhumed (MacLeod et al., 2002; Ranero, et al., 1999; Tucholke et al., 1998; Blackman et al., 1998; Mutter and Karson, 1992). On Macquarie Island, no detachment fault has been observed capping the exposed lower-crustal rocks, and the mylonites adjacent to Finch-Langdon fault segments show steep dips and down-dip stretching lineations, suggesting they represent earlier movement on the same high-angle faults but at deeper levels (Wertz, 2003). A detachment, however, easily could have been eroded during uplift of the island as the surface reached wave base; if truncated by the high-angle, spreading-related faults, no vestiges would be expected to remain. Thus, we cannot rule out that the deeper crustal rocks were primarily exhumed by a detachment fault that is no longer exposed. The high-angle Finch-Langdon faults were clearly active during sedimentation, however, as discussed above. Additionally, the rotation of the sedimentary rocks into near-vertical to overturned orientations with younging away from the faults (i.e., "drag") indicates that motion postdated at least some of the sedimentation. The potentially listric Major Lake and Caroline Cove–Windsor Bay faults that show sedimentary rocks younging and dipping toward the fault have much less throw but could sole in a lower unexposed detachment. Thus, Macquarie Island exposures suggest that the high-angle faults at inside corners have the most pronounced influence on sedimentation. Although it is likely that sedimentation was dominantly toward the ridge-transform intersection as observed on the seafloor (Blackman et al., 1998), our results also suggest that significant transport could be away from the inside corner highs.

Recently, Rivizzigno and Karson (2004) proposed that Macquarie Island crust formed during an interval of oblique spreading along east-trending spreading segments punctuated by a series of northwest-trending discontinuities that include the Finch-Langdon, Major Lake, and Caroline Cove–Windsor Bay faults discussed here. In their model, these fault zones have a graben-like morphology and represent accommodation zones that formed during extremely oblique spreading. The sedimentary rock distribution on Macquarie Island, however, does not support a graben-like morphology for these northwest-trending fault zones (cf. Fig. 3 of Rivizzigno and Karson, 2004), especially those adjacent to the Finch-Langdon fault zone. Furthermore, the majority of sedimentary rocks near to Major Lake lie outside and north of the graben-like structure mapped by Rivizzigno and Karson (2004). Our data indicate that the northwest-trending fault zones are defined by fault scarps that shed sediment mainly toward the south and west; we see no evidence for there having been two sides of a graben-like valley. We also point out that new geophysical data (Bernardel and Symonds, 2001) collected directly east of Macquarie Island indicate a north-northeast-striking fracture zone ~7 km offshore, and west-northwest-striking spreading fabric (abyssal hill faults), which does not support the assertion made by Rivizzigno and Karson (2004) that the northwest-trending fault zones parallel offshore lineaments identified as fracture zones.

CONCLUSIONS

Upper Miocene to lower Pliocene breccia, sandstone, and siltstone composed of oceanic crustal material form extensive turbidity-current–generated debris fans deposited in an active tectonic environment adjacent to major relict seafloor spreading faults on Macquarie Island. Pillow lava and massive basalt flows are interbedded with the sedimentary rocks, showing that faulting, sedimentation, and volcanism were contemporaneous. Fault-zone gouge in major relict seafloor spreading faults, such as the Finch-Langdon fault, is similar in type, size, and mineralogy to clastic material identified in nearby sedimentary rocks, indicating that most sedimentary rocks on Macquarie Island were produced by the physical disintegration and tectonic abrasion of oceanic crust in fault zones and mass wasting of such tectonic features. Sedimentary structures indicate that small-scale turbidity currents were the dominant sediment gravity flow mechanism. Diabase and gabbro clasts in some sedimentary rocks indicate that middle and lower oceanic crust were exposed to erosion on the seafloor. Spatial relationships between sedimentary rocks and major relict high-angle seafloor spreading faults both onshore and offshore support the formation of the Finch-Langdon fault in an inside corner of a ridge-transform intersection and demonstrate the dominant influence of such faults on sedimentation in these environments.

ACKNOWLEDGMENTS

We are grateful to the Australian Antarctic Science Advisory Committee (ASAC), the Australian National Antarctic Research Expeditions (ANARE), the Australian Antarctic Division, University of Texas Geology Foundation, and the Japanese Ministry of Education, Culture, Sports, Science, and Technology (MEXT) for their support of this research. Plate tectonic reconstructions were undertaken under the auspices of the PLATES project at the University of Texas Institute for Geophysics (UTIG); L. Gahagan provided able technical support and scientific insight. Constructive reviews by P. Cawood and two anonymous reviewers, and careful editorial work by N. Riggs helped improve the manuscript. We thank the expeditioners of the 53rd and 55th ANARE, including Karah Wertz, for their assistance in the field. This is UTIG contribution number 1645.

REFERENCES CITED

Allerton, S., and Vine, F.J., 1992, Deformation styles adjacent to transform faults: evidence from the Troodos Ophiolite, Cyprus, *in* Parson, L.M., et al., eds., Ophiolites and their modern oceanic analogues: London, Geological Society Special Publication 60, p. 251–261.

Barany, I., and Karson, J.A., 1989, Basaltic breccias of the Clipperton fracture zone (east Pacific): Sedimentation and tectonics in a fast-slipping oceanic transform: Geological Society of America Bulletin, v. 101, p. 204–220, doi: 10.1130/0016-7606(1989)1012.3.CO;2.

Bernardel, G., and Symonds, P.A., 200l, Seafloor mapping of the southeast region and adjacent waters – AUSTREA final report: Southern Macquarie Ridge: Australian Geological Survey Organisation Record, v. 200l, no. 46, p. 25.

Bertrand, J., Nievergelt, P., and Vuagnat, M., 1984, Oceanic sedimentary processes and alpine metamorphic events in the Montgenevre ophiolite, western Alps: Ofioliti, v. 9, p. 303–320.

Blackman, D.K., Cann, J.R., Janssen, B., and Smith, D.K., 1998, Origin of extensional core complexes: Evidence from the Mid-Atlantic Ridge at Atlantis Fracture Zone: Journal of Geophysical Research, v. 103, p. 21,315–21,334, doi: 10.1029/98JB01756.

Bouma, A.H., 1962, Sedimentology of some Flysch deposits; a graphic approach to facies interpretation: Amsterdam, Elsevier, 168 p.

Cande, S.C., and Stock, J.M., 2004, Pacific-Antarctic-Australia motion and the formation of the Macquarie Plate: Geophysical Journal International, v. 157, p. 399–414, doi: 10.1111/J.1365-246X.2004.02224.X.

Cande, S.C., Stock, J.M., Muller, R.D., and Ishihara, T., 2000, Cenozoic motion between east and west Antarctica: Nature, v. 404, p. 145–150, doi: 10.1038/35004501.

Cann, J.R., Blackman, D.K., Smith, D.K., McAllister, E., Janssen, B., Mello, S., Avgerinos, E., Pascoe, A.R., and Escartin, J., 1997, Corrugated slip surfaces formed at ridge-transform intersections on the Mid-Atlantic Ridge: Nature, v. 385, p. 329–332, doi: 10.1038/385329A0.

Cannat, M., 1993, Emplacement of mantle rocks in the seafloor at mid-ocean ridges: Journal of Geophysical Research, v. 98, p. 4,163–4,172.

Christodoulou, C., Griffin, B.J., and Foden, J., 1984, The geology of Macquarie Island: Hobart, Tasmania, Australia, Australian National Antarctic Research Expeditions research notes 21, 15 p.

Daczko, N.R., Wertz, K.L., Mosher, S., Coffin, M.F., and Meckel, T.A., 2003, Extension along the Australian-Pacific transpressional transform plate boundary near Macquarie Island: Geochemistry, Geophysics, Geosystems, v. 4(9), p. 1–22, doi: 10.1029/ 2003GC000523.

Duncan, R.A., and Varne, R., 1988, The age and distribution of the igneous rocks of Macquarie Island: Papers and Proceedings of the Royal Society of Tasmania, v. 122, p. 45–50.

Fox, P.J., and Gallo, D.G., 1984, Tectonic model for ridge-transform-ridge plate boundaries: Implications for the

structure of oceanic lithosphere: Tectonophysics, v. 104, p. 205–242, doi: 10.1016/0040-1951(84)90124-0.

Frohlich, C., Coffin, M.F., Massell, C.G., Mann, P., Schuur, C.L., Davis, S.D., Jones, T., and Karner, G., 1997, Constraints on Macquarie Ridge tectonics provided by Harvard focal mechanisms and teleseismic earthquake locations: Journal of Geophysical Research, v. 102, p. 5,029–5,041, doi: 10.1029/96JB03408.

Gallo, D.G., Kidd, W.S.F., Fox, P.J., Karson, K.A., Macdonald, K., Crane, K., Choukroune, P., Seguret, M., Moody, R., and Kastens, K., 1984, Tectonics at the intersection of the East Pacific rise with Tamayo transform fault: Marine Geophysical Researches, v. 6, p. 159–185.

Goscombe, B.D., and Everard, J.L., 1998, Macquarie Island mapping reveals three tectonic phases: Eos (Transactions, American Geophysical Union), v. 80, p. 50, 55.

Goscombe, B.D., and Everard, J.L., 2001, Tectonic evolution of Macquarie Island; extensional structures and block rotations in oceanic crust: Journal of Structural Geology, v. 23, p. 639–673, doi: 10.1016/S0191-8141(00)00141-3.

Karson, J.A., 1984, Variations in structure and petrology in the Coastal complex, Newfoundland: Anatomy of an oceanic fracture zone, *in* Gass, I.G., Lippard, S.J., and Shelton, A.W., eds., Ophiolites and oceanic lithosphere: Geological Society [London] Special Publication 13, p. 131–144.

Karson, J.A., and Dick, H.J.B., 1983, Tectonics of ridge-transform intersections at the Kane fracture zone: Marine Geophysical Researches, v. 6, p. 51–98.

Karson, J.A., Fox, P.J., Sloan, H., Crane, K.T., Kidd, W.S.F., Bonatti, E., Stroup, J.B., Fornari, D.J., Elthon, D., Hamlyn, P., Casey, J.F., Gallo, D.G., Needham, D., and Sartori, R., 1984, The geology of the oceanographer transform: The ridge-transform intersection: Marine Geophysical Researches, v. 6, p. 109–141.

Lagabrielle, Y., and Cannat, M., 1990, Alpine Jurassic ophiolites resemble the modern central Atlantic basement: Geology, v. 18, p. 319–322, doi: 10.1130/0091-7613(1990)0182.3.CO;2.

Lagabrielle, Y., Bideau, D., Cannat, M., Karson, J.A., and Mevel, C., 1998, Ultramafic-mafic plutonic rock suites exposed along the Mid-Atlantic Ridge (10 degrees N-30 degrees N); symmetrical-asymmetrical distribution and implications for seafloor spreading processes, *in* Buck, W.R., Delaney, P., Karson, J.A., Lagabrielle, Y., eds., Faulting and magmatism at mid-ocean ridges: American Geophysical Union Geophysical Monograph 106, p. 153–176.

Lamarche, G., Collot, J.-Y., Wood, R.A., Sosson, M., Sutherland, R., and Delteil, J., 1997, The Oligocene-Miocene Pacific-Australian plate boundary, south of New Zealand: Evolution from oceanic spreading to strike-slip faulting: Earth and Planetary Science Letters, v. 148, p. 129–139, doi: 10.1016/S0012-821X(97)00026-5.

Lawver, L.A., Coffin, M.F., Dalziel, I.W.D., Gahagan, L.M., and Campbell, D.A., 2001, The Plates 2001 atlas of plate reconstructions (750 Ma to present day), Plates Progress Report No. 260–0801: UTIG Technical Report No. 189, p. 83.

Lowe, D.R., 1982, Sediment gravity flows II, Depositional models with special references to the deposits of high-density turbidity currents: Journal of Sedimentary Petrology, v. 52, p. 279–297.

MacLeod, C.J., Allerton, S., Gass, I.G., and Xenophontos, C., 1990, Structure of a fossil ridge-transform intersection in the Troodos Ophiolite: Nature, v. 348, p. 717–720, doi: 10.1038/348717A0.

MacLeod, C.J., Escartin, J., Banerji, D., Banks, G.J., Gleeson, M., Irving, D.H.B., Lilly, R.M., McCaig, A.M., Niu, Y., Allerton, S., and Smith, D.K., 2002, Direct geological evidence for oceanic detachment faulting: The Mid-Atlantic Ridge, 15°45'N: Geology, v. 30, p. 879–883, doi: 10.1130/0091-7613(2002)0302.0.CO;2.

Massell, C., Coffin, M.F., Mann, P., Mosher, S., Frohlich, C., Schuur, C.L., Karner, G.D., Ramsay, D., and Lebrun, J.F., 2000, Neotectonics of the Macquarie Ridge Complex, Australia-Pacific plate boundary: Journal of Geophysical Research, v. 105, p. 13,457–13,480, doi: 10.1029/1999JB900408.

Meckel, T.A., 2003, Tectonics of the Hjort region of the Macquarie Ridge Complex, southernmost Australian-Pacific Plate Boundary, southwest Pacific Ocean [Ph.D. thesis]: Austin, University of Texas, 192 p.

Mitchell, N.C., Tivey, M.A., and Gente, P., 2000, Seafloor slopes at mid-ocean ridges from submersible observations and implications for interpreting geology from seafloor topography: Earth and Planetary Science Letters, v. 183, p. 543–555, doi: 10.1016/S0012-821X(00)00270-3.

Moores, E.M., and Vine, F.J., 1971, The Troodos massif, Cyprus and other ophiolites as oceanic crust; evaluation and implications, a discussion on the petrology of igneous and metamorphic rocks from the ocean floor: Philosophical Transactions of the Royal Society of London, Series A: Mathematical and Physical Sciences, v. 268, p. 443–466.

Mutter, J.C., and Karson, J.A., 1992, Structural processes at slow-spreading ridges: Science, v. 257, p. 627–634.

Quilty, P.G., Rubenach, M., and Wilcoxon, J.A., 1973, Miocene Ooze from Macquarie Island: Search Sydney, v. 4, p. 163–164.

Rivizzigno, P.A., and Karson, J.A., 2004, Structural expression of oblique seafloor spreading in the Macquarie Island ophiolite, Southern Ocean: Geology, v. 32, p. 125–128, doi: 10.1130/G19906.1.

Sandwell, D.T., and Smith, W.H.F., 1997, Marine gravity anomaly from Geosat and ERS 1 satellite altimetry: Journal of Geophysical Research, v. 102, p. 10,039–10,054, doi: 10.1029/96JB03223.

Schroeder, T., John, B., and Frost, B.R., 2002, Geologic implications of seawater circulation through peridotite exposed at slow-spreading mid-ocean ridges: Geology, v. 30, p. 367–370, doi: 10.1130/0091-7613(2002)0302.0.CO;2.

Severinghaus, J., and MacDonald, K., 1988, High inside corners at ridge-transform intersections: Marine Geophysical Researches, v. 9, p. 353–367.

Simonian, K., and Gass, I.G., 1978, Arakapas fault belt, Cyprus, a fossil transform fault: Geological Society of America Bulletin, v. 89, p. 1,220–1,230.

Thy, P., and Yildirim, D., 2000, Magmatic and tectonic controls on the evolution of oceanic magma chambers at slow-spreading ridges; perspectives from ophiolitic and continental layered intrusions, *in* Dilek, Y., Moores, E.M., Elthon, D., Nicolas, A., eds., Ophiolites and oceanic crust; new insights from field studies and the Ocean Drilling Program: Geological Society of America Special Paper 349, p. 87–104.

Tucholke, B.E., and Lin, J., 1994, A geological model for the structure of ridge segments in slow-spreading ocean crust: Journal of Geophysical Research, v. 99, p. 11,937–11,958.

Tucholke, B.E., Lin, J., and Kleinrock, M.C., 1998, Megamullions and mullion structure defining oceanic metamorphic core complexes on the Mid-Atlantic Ridge: Journal of Geophysical Research, v. 103, p. 9,857–9,866, doi: 10.1029/98JB00167.

Varne, R., and Rubenach, M.J., 1972, Geology of Macquarie Island in relation to tectonic environment, *in* Hayes, D.E., ed., Antarctic oceanology II: The Australian-New Zealand sector: American Geophysical Union Antarctic Research Series 19, p. 535–541.

Varne, R., Gee, R.D., and Quilty, P.G.J., 1969, Macquarie island and the cause of oceanic linear magnetic anomalies: Science, v. 166, p. 230–233.

Varne, R., Brown, A.V., and Falloon, T., 2000, Macquarie Island; its geology, structural history, and the timing and tectonic setting of its N-MORB to E-MORB magmatism, *in* Dilek Y., et al., eds., Ophiolites and oceanic crust; new insights from field studies and the Ocean Drilling Program: Geological Society of America Special Paper 349, p. 301–320.

Weissel, J.K., Hayes, D.E., and Herron, E.M., 1977, Plate tectonics synthesis: The displacements between Australia, New Zealand, and Antarctica since the late Cretaceous: Marine Geology, v. 25, p. 231–277, doi: 10.1016/0025-3227(77)90054-8.

Wertz, K.L., 2003, From seafloor spreading to uplift: The structural and geochemical evolution of Macquarie Island on the Australian-Pacific plate boundary [Ph.D. thesis]: Austin, University of Texas, 189 p.

Wertz, K.L., Snow, J.E., Hellebrand, E., von der Handt, A., and Mosher, S., 2002, Depleted peridotites of Macquarie Island, an uplifted section of in-situ oceanic crust: Eos (Transactions, American Geophysical Union), 83(47), Fall Meeting Supplement, Abstract V52A–1284.

Wertz, K.L., Mosher, S., Daczko, N.R., and Coffin, M.F., 2003, Macquarie Island's Finch-Langdon fault: A ridge-transform inside corner structure: Geology, v. 31, p. 661–664, doi: 10.1130/G19441.1.

Wood, R., Lamarche, G., Herzer, R., Delteil, J., and Davy, B., 1996, Paleogene seafloor spreading in the southeast Tasman Sea: Tectonics, v. 15, p. 966–975, doi: 10.1029/96TC00129.

Manuscript Received by the Society 12 August 2003
Revised Manuscript Received 9 May 2004
Manuscript Accepted 2 June 2004

Printed in the USA